

## THE $M_{\text{BH}}\text{-}\sigma$ DIAGRAM, AND THE OFFSET NATURE OF BARRED ACTIVE GALAXIES

ALISTER W. GRAHAM<sup>1</sup> AND I-HUI LI

Centre for Astrophysics and Supercomputing, Swinburne University of Technology, Hawthorn, Victoria 3122, Australia.  
*accepted for publication in ApJ, March 16, 2009*

### ABSTRACT

From a sample of 50 predominantly inactive galaxies with direct supermassive black hole mass measurements, it has recently been established that barred galaxies tend to reside rightward of the  $M_{\text{bh}}\text{-}\sigma$  relation defined by non-barred galaxies. Either black holes in barred galaxies tend to be anaemic or the central velocity dispersions in these galaxies have a tendency to be elevated by the presence of the bar. The latter option is in accord with studies connecting larger velocity dispersions in galaxies with old bars, while the former scenario is at odds with the observation that barred galaxies do not deviate from the  $M_{\text{bh}}\text{-luminosity}$  relation. Using a sample of 88 galaxies with active galactic nuclei, whose supermassive black hole masses have been estimated from their associated emission lines, we reveal for the first time that they also display this same general behavior in the  $M_{\text{bh}}\text{-}\sigma$  diagram depending on the presence of a bar or not. A new symmetrical and non-symmetrical “barless”  $M_{\text{bh}}\text{-}\sigma$  relation is derived using 82 non-barred galaxies. The barred galaxies are shown to reside on or up to  $\sim 1$  dex below this relation. This may explain why narrow-line Seyfert 1 galaxies appear offset from the “barless”  $M_{\text{bh}}\text{-}\sigma$  relation, and has far reaching implications given that over half of the disk galaxy population are barred.

*Subject headings:* black hole physics — galaxies: active — galaxies: nuclei — galaxies: Seyfert — galaxies: structure

### 1. INTRODUCTION

Black holes fascinate astronomers and the general public alike due to their extreme physical conditions. How the supermassive variety came to be at the centres of most, if not all, massive galaxies has been the focus of increased research over recent years. Valuable clues are thought to reside within the observed scaling laws involving the mass of the central black hole,  $M_{\text{bh}}$ , and various properties of the host galaxy (e.g., Ferrarese & Ford 2005 and references therein). Indeed, the low level of scatter within these relations suggests a direct physical connection between the black hole and the host galaxy; although which parameters are doing the driving, or are merely along for the ride, remains unclear (Novak et al. 2006).

One well known scaling law involves the velocity dispersion,  $\sigma$ , of the host galaxy (Ferrarese & Merritt 2000; Gebhardt et al. 2000). With parameter measurement errors initially of comparable size to the total root mean square (r.m.s.) scatter about the  $M_{\text{bh}}\text{-}\sigma$  relation, this scaling law was heralded as a potential fundamental relation with zero intrinsic scatter (Ferrarese & Merritt 2000). If correct, it would imply that the host galaxy’s velocity dispersion controls the growth of supermassive black holes (SMBHs), and is the physical property which theorists should concentrate their efforts on. The situation did however become more interesting, if not complicated, when Graham (2007; 2008a,b) and Hu (2008) revealed the presence of substructure within the  $M_{\text{bh}}\text{-}\sigma$  plane. They discovered that the location of a galaxy/black hole pair in this diagram depends on whether or not the galaxy is barred (or has a “pseudobulge” in Hu’s presentation). Moreover, the offset of

barred galaxies from the “barless  $M_{\text{bh}}\text{-}\sigma$  relation” can be up to  $\sim 1$  dex in the log  $M_{\text{bh}}$  direction.

Graham (2008a) suggested that the radial orbits of stars in bars may lead to an enhanced velocity dispersion measurement when one is looking down (some component of) the length of a bar. In addition, bars which have evolved for a sufficient amount of time are expected to increase their galaxy’s central velocity dispersion, even in face on galaxies (Gadotti & de Souza 2005, and references therein). Indeed, bars with an older stellar population have been observed to possess higher velocity dispersions than younger bars (Perez et al. 2009). This will contribute to, if not explain, the discrepant behavior of barred galaxies in the  $M_{\text{bh}}\text{-}\sigma$  diagram. Alternatively or additionally, the supermassive black holes in barred galaxies may be relatively malnourished compared to those in barless galaxies. That is, perhaps they are still being fuelled/fed by the bar<sup>2</sup> and as such are yet to reach the barless  $M_{\text{bh}}\text{-}\sigma$  relation (Mathur & Grupe 2005a; Zhou et al. 2006). However, if this were true, then the barred galaxies would also be outliers in the  $M_{\text{bh}}\text{-luminosity}$  diagram, yet data to date suggests that they are not (Graham 2008a; Bentz et al. 2009).

Ferrarese et al. (2001, see also Wang & Lu 2001) have shown that black holes in AGN roughly abide by the  $M_{\text{bh}}\text{-}\sigma$  relation defined by quiescent galaxies. In this paper we explore the demographics within the  $M_{\text{bh}}\text{-}\sigma$  plane by including a sample of 88 active galactic nuclei (AGN). Specifically, we address the question of whether or not, at a fixed black hole mass, do barred galaxies (with AGN) have a tendency to possess greater velocity dispersions than non-barred galaxies (with AGN). In Section 2 we present the galaxy sample, and our method of image

<sup>1</sup> Corresponding Author: AGraham@swin.edu.au

<sup>2</sup> We note that it is not clear whether bars funnel gas all the way to the center of their galaxies, e.g. Forbes et al. 1994.

analysis to determine if a bar may be present. Images for the full AGN galaxy sample are available electronically. In Section 3 we show the location of the barred and non-barred galaxies within the  $M_{\text{bh}}-\sigma$  diagram. Galaxies with AGN are revealed, for the first time, to follow the same distributions as inactive barred and unbarred galaxies. That is, barred AGN reside up to 1 dex in the  $\log M_{\text{bh}}$  direction below the barless  $M_{\text{bh}}-\sigma$  relation. Our main conclusions are presented in Section 4.

## 2. DATA

Broad emission-line reverberation-mapping data was used by Peterson et al. (2004) to acquire SMBH virial masses for 35 AGN, which were subsequently used to calibrate a number of scaling relations for estimating SMBH masses in other AGN (e.g., Greene & Ho 2005; Kaspi et al. 2005). Here we have used Greene & Ho’s (2006, their Table 1) useful list of 88 local active galaxies with stellar velocity dispersion measurements and estimated black hole masses.<sup>3</sup> Such estimates are typically considered accurate to within a factor of 3-4 (e.g., Krolik 2001; Metzroth et al. 2006; Vestergaard & Peterson 2006). We then determined if a bar is present or not in these galaxies.

Images for the 88 AGN have predominantly been taken from the Sloan Digital Sky Survey (SDSS; Abazajian et al. 2008 and references therein), with the remaining images obtained via the NASA Extragalactic Database (NED). While a visual inspection of the images can, and often does, reveal bars in many galaxies, it also leaves some ambiguous cases. To help address these we have subtracted from the original image a number of smoothed representations. Sometimes this smoothed version was an elliptical object with the same median ellipticity and position angle as the galaxy, while other times it was a Gaussian smoothed version of the original image. This common technique (e.g., Jerjen et al. 2000; Yuan et al. 2001, Erwin & Sparke 2002) created a set of residual images which can more clearly reveal non-symmetrical structures such as stellar bars. A couple of example images are shown in Figure 1, and a complete set of images for all 88 galaxies is available electronically. In addition we used the IRAF task ELLIPSE to generate ellipticity and position angle profiles, which were found to be helpful in identifying/confirming the presence of bars. This was typically signalled by a high ellipticity over the inner regions once the bar light starts to dominate; the ellipticity profile would then decline with increasing radius while often accompanied by a changing position angle as the outer disk comes into dominance (Figure 2).

In Table 1 we have identified which galaxies appear to have bars or not. For some galaxies we were left uncertain as to whether what appeared to be a bar was real, and we have assigned these with the status “maybe”. A “no” signals that we saw no evidence for a bar. While this system may sound obvious, it is worth clarifying that poorly resolved or edge-on systems in which a bar might

exist but for which we saw no evidence are designated as “no” rather than “maybe”. Given our suspicion that the outlying galaxies in the  $M_{\text{bh}}-\sigma$  diagram are barred, a stronger test of our hypothesis would therefore involve such an economical assignment of bars. We have however denoted five galaxies (NGC 3227, 3516, 3783, 4151, and 7469) to be barred given their designation as such by others, according to NED, although this was not clear from the SDSS images. From the 88 AGN we were able to positively (tentatively) identify 26 (16) barred galaxies, giving a *total* fraction of 42/88 which is roughly half of the sample. We do however note that for twenty small and faint galaxies with  $\sigma < 85 \text{ km s}^{-1}$ , it was hard to detect the presence of a bar and all but one have been tabulated as having no (detectable) bar.

<sup>3</sup> Although the normalization (from the scaling factor  $f$  pertaining to the broad line region’s geometry and kinematics) of these SMBH masses is tied to the  $M_{\text{bh}}-\sigma$  relation of inactive galaxies (Onken et al. 2004), “circular rationale” should not be the cause of the barred and unbarred AGN potentially occupying the same distribution and locus as barred and unbarred inactive galaxies in the  $M_{\text{bh}}-\sigma$  plane.

TABLE 1  
GALAXY PROPERTIES

Gal. Id.	CDS Name	R.A. [Deg]	Dec. [Deg]	Classification	$\epsilon$	Bar
(1)	(2)	(3)	(4)	(5)	(6)	(7)
1	SDSS J000805.62+145023.4	2.02333	14.83972	Sy1	0.41	yes
2	SDSS J004236.86-104921.8	10.65417	-10.81000	Sy1.5	0.18	maybe
3	SDSS J010712.03+140844.9	16.80000	14.14583	NLSy1?	0.05	no
4	SDSS J011703.58+000027.3	19.26500	0.00750	NLSy1	0.29	yes
5	SDSS J020459.25-080816.0	31.24687	-8.13778	...	0.45	yes
6	SDSS J020615.99-001729.1	31.56708	-0.29139	S0;merger?	0.50	no
7	SDSS J021011.49-090335.5	32.54787	-9.05986	Sa	0.38	yes
8	SDSS J021257.59+140610.1	33.23996	14.10281	BLAGN	0.40	no
9	Mrk 590	33.64000	-0.76667	SA(s)a	0.12	no
10	SDSS J024912.86-081525.6	42.30375	-8.25722	BLAGN	0.25	no
11	SDSS J032515.59+003408.4	51.31500	0.56889	...	0.10	no
12	SDSS J033013.26-053236.0	52.55500	-5.54333	Sb	0.40	maybe
13	3C 120	68.29625	5.35444	S0;LPG;BLRG;	0.40	maybe
14	Akn 120	79.04792	-0.15028	Sb/pec	0.99	no
15	Mrk 79	115.63708	49.80917	SBb	0.50	yes
16	SDSS J075057.25+353037.5	117.73854	35.51042	...	0.99	no
17	SDSS J080243.39+310403.3	120.68083	31.06750	AGN	0.18	no
18	SDSS J080538.66+261005.4	121.41125	26.16806	SB(s)bc	0.30	yes
19	SDSS J080907.58+441641.4	122.28167	44.27806	Sy	0.20	no
20	SDSS J082510.23+375919.7	126.29250	37.98889	...	0.65	maybe
21	SDSS J082912.67+500652.3	127.30292	50.11444	BLAGN	0.10	no
22	SDSS J083202.16+461425.7	128.00500	46.24389	Sy1	0.20	yes
23	SDSS J083949.64+484701.4	129.95750	48.78361	Sy1	0.25	maybe
24	SDSS J085554.27+005110.9	133.97612	0.85303	Sy1	0.40	no
25	SDSS J092438.88+560746.9	141.16375	56.12861	NLSy1	0.50	yes
26	Mrk 110	141.30375	52.28639	Pair?	0.99	no
27	SDSS J093259.60+040506.0	143.24833	4.08500	...	0.03	maybe
28	SDSS J093812.26+074340.0	144.55125	7.72778	...	0.20	no
29	SDSS J094838.42+403043.7	147.16000	40.51222	Sy	0.50	yes
30	SDSS J101108.40+002908.7	152.78500	0.48583	...	0.15	no
31	SDSS J101627.32-000714.5	154.11375	-0.12056	...	0.35	no
32	SDSS J101912.57+635802.7	154.80250	63.96750	E;Sy1.5	0.40	yes
33	SDSS J102044.43+013048.4	155.18512	1.51344	BLAGN	0.10	no
34	NGC 3227	155.87750	19.86500	SAB(s)	0.60	yes
35	SDSS J110640.20+051905.6	166.66750	5.31822	...	0.25	yes
36	NGC 3516	166.69833	72.56889	(R)SB(s)0	0.27	yes
37	SDSS J112536.16+542257.1	171.40083	54.38167	S0	0.55	no
38	SDSS J112841.00+575006.5	172.17083	57.83514	Sy2	0.34	yes
39	NGC 3783	174.75750	-37.73861	(R')SB(r)a	0.15	yes
40	POX 52	180.73708	-20.93417	...	0.45	no
41	SDSS J120257.81+045045.0	180.74083	4.84583	(R')SA(s)c:	0.50	maybe
42	NGC 4051	180.79000	44.53139	SAB(rs)bc	0.55	yes
43	SDSS J120556.01+495956.1	181.48337	49.99892	...	0.18	no
44	NGC 4151	182.63625	39.40556	(R')SAB(rs)ab	0.50	yes
45	SDSS J121607.09+504930.0	184.02958	50.82500	SBb?	0.66	yes
46	SDSS J121754.97+583935.6	184.47917	58.66000	compact	0.21	no
47	SDSS J122324.13+024044.4	185.85042	2.67917	E?	0.35	no
48	NGC 4395	186.45375	33.54667	SA(s)m;LINER	0.15	no
49	SDSS J123237.48+662452.3	188.15583	66.41444	BLAGN	0.40	no
50	SDSS J124035.81-002919.4	190.14917	-0.48861	AGN	0.05	no
51	SDSS J125055.28-015556.6	192.73042	-1.93250	AGN	0.10	no
52	SDSS J130620.97+531823.1	196.58750	53.30639	...	0.25	no
53	SDSS J131305.80+012755.9	198.27417	1.46556	BLAGN	0.08	maybe
54	SDSS J132249.21+545528.2	200.70504	54.92450	Sy1.5	0.40	no
55	SDSS J132340.31-012749.2	200.91796	-1.46367	Sy1.5	0.10	no
56	SDSS J134952.84+020445.1	207.47000	2.07917	Sy1	0.50	maybe
57	Mrk 279	208.26458	69.30806	S0	0.34	no
58	SDSS J140018.42+050242.2	210.07667	5.04500	...	0.28	maybe
59	SDSS J140514.87-025901.2	211.31196	-2.98367	...	0.55	yes
60	SDSS J141630.81+013708.0	214.12837	1.61889	BLAGN	0.30	maybe
61	NGC 5548	214.49875	25.13694	(R')SA(s)0/a	0.20	no
62	SDSS J143450.62+033842.5	218.71125	3.64444	Sc	0.12	maybe
63	SDSS J143452.45+483942.7	218.71875	48.66194	SB(s)0/a?	0.10	no
64	Mrk 817	219.09250	58.79417	SBc	0.10	yes
65	SDSS J144629.97+500130.5	221.62500	50.02528	...	0.22	no
66	SDSS J145706.80+494008.4	224.27833	49.66917	SB(s)b	0.10	maybe
67	SDSS J145901.35+611353.5	224.75542	61.23139	S	0.38	yes
68	SDSS J150556.55+034226.3	226.48562	3.70731	Sa/b	0.50	maybe
69	SDSS J150745.00+512710.2	226.93750	51.45278	Sy1	0.65	yes
70	SDSS J150853.95-001148.9	227.22479	-0.19692	Compact	0.20	no

TABLE 1  
GALAXY PROPERTIES *cont.*

(1)	(2)	CDS Name	R.A. [Deg] (3)	Dec. [Deg] (4)	Classification (5)	$\epsilon$ (6)	Bar (7)
71		SDSS J152515.18+601409.0	231.31325	60.25833	Sy2	0.08	maybe
72		SDSS J155417.43+323837.8	238.57262	32.64383	AGN	0.15	maybe
73		SDSS J161156.31+521116.8	242.98458	52.18806	BLAGN	0.30	no
74		SDSS J161951.31+405847.2	244.96375	40.97944	SBab	0.60	yes
75		SDSS J170246.09+602818.9	255.69208	60.47194	...	0.16	no
76		SDSS J170328.96+614109.9	255.87083	61.68611	BLAGN	0.99	no
77		SDSS J171550.49+593548.7	258.96037	59.59686	BLAGN	0.50	yes
78		SDSS J172759.15+542147.0	261.99625	54.36306	NLSy1?	0.15	no
79		3C 390.3	280.53750	79.77139	BLRG	0.20	no
80		SDSS J212401.90-002158.7	321.00792	-0.36603	AGN	0.99	no
81		SDSS J215658.30+110343.1	329.24292	11.06194	Sy	0.30	yes
82		SDSS J222435.29-001103.8	336.14708	-0.18444	...	0.15	no
83		SDSS J223000.37-094622.1	337.50154	-9.77281	...	0.30	no
84		NGC 7469	345.81583	8.87389	(R')SAB(rs)a	0.33	yes
85		SDSS J232159.06+000738.8	350.49625	0.12750	...	0.35	no
86		SDSS J232721.96+152437.3	351.84167	15.41028	Sy1	0.25	no
87		SDSS J233837.10-002810.3	354.65458	-0.46944	NLAGN	0.99	no
88		SDSS J235128.78+155259.0	357.86992	15.88306	AGN	0.45	no

NOTE. — Col. (1): Running galaxy identification number. Col. (2): Galaxy name from the Centre de Données astronomiques de Strasbourg (CDS)<sup>a</sup>. Col. (3): Right Ascension. Col. (4): Declination. Col. (5): Classification in the NASA Extragalactic Database (NED)<sup>b</sup>. Col. (6): (IRAF/ELLIPSE)-determined ellipticity,  $\epsilon$ , of the outer isophotes — indicative of the galaxy inclination for the disk galaxies. Col. (7): Whether or not a bar was detected. Black hole masses and velocity dispersions are tabulated in Greene & Ho (2006, their Table 1).

<sup>a</sup><http://cdsweb.u-strasbg.fr>

<sup>b</sup><http://nedwww.ipac.caltech.edu>

### 3. RESULTS

Figure 3 reveals the location of the 88 galaxies with AGN in the  $M_{\text{bh}}-\sigma$  plane. For clarity we have not plotted error bars here, but they can be seen in Graham (2008b).

#### 3.1. Inactive galaxies

To set the context, shown in Figure 3a) is a local sample of 50 predominantly inactive galaxies for which direct supermassive black hole mass measurements have been catalogued (Graham 2008b). Of these 50 galaxies, 28 are disk galaxies, and 14 are barred. That is, half of the disk galaxies are barred, which is in fair agreement with optical studies of the bar fraction in spiral galaxies. For example, Knapen et al. (2000, see also Marinova & Jogee 2007, and Hernández-Toledo et al. 2008; and Weinzirl et al. 2009) have reported that  $\sim 60\%$  of disk galaxies have bars, although it may be as high as 75% (e.g., Eskridge et al. 2000). These barred galaxies are denoted by crosses in Figure 3a) and they clearly display the reported tendency to reside on or below the  $M_{\text{bh}}-\sigma$  relation defined by the non-barred galaxies. The “barless  $M_{\text{bh}}-\sigma$  relation” shown in Figure 3a) by the solid straight line was obtained by Graham (2008b) using the (symmetrical) bisector linear regression routine BCES from Akritas & Bershady (1996), and assuming a 10% uncertainty on the velocity dispersion values. The relation is such that  $\log(M_{\text{bh}}/M_{\odot}) = (8.25 \pm 0.05) + (4.39 \pm 0.32) \log[\sigma/200 \text{ km s}^{-1}]$ . The dashed lines in this panel reflect the  $1\sigma$  uncertainty on the slope and intercept of this relation, while the shaded area expands this boundary by 0.33 dex (the r.m.s. scatter in the  $\log M_{\text{bh}}$  direction about the  $M_{\text{bh}}-\sigma$  relation for the non-barred galaxies).

Given concerns from different corners about potential biases with some regression techniques, we have checked the above relation using two additional codes. First, we have used Tremaine et al.’s (2002) modified version of the routine FITEXY (Press et al. 1992, their Section 15.3) to construct two relations: one which minimised the scatter in the  $\log M_{\text{bh}}$  direction and another which minimised the scatter in the  $\log \sigma$  direction (see Novak et al. 2006). Averaging these two relations gives a slope and intercept of  $(4.17 + 4.67)/2 = 4.42$  and  $(8.26 + 8.26)/2 = 8.26$ , respectively. The second code which we have used is an IDL routine from Kelly (2007) which employs a Bayesian method to account for measurement errors. The median solution (plus/minus 34%) from the distribution of 10000 simulations has a slope and intercept of  $4.39 \pm 0.35$  and  $8.26 \pm 0.06$  respectively, and is therefore consistent with our two other symmetrical regression analyses for this data.

#### 3.2. All galaxies

Figures 3b) and 3c) include both the inactive and active galaxies. A few galaxies stand out and may be worthy of identification. For example, the barred galaxy in the lower-left of Figure 3c) (with  $M_{\text{bh}} = 4 \times 10^9 M_{\odot}$  and  $\sigma = 48 \text{ km s}^{-1}$ ) is galaxy number 62 (see Table 1), a face-on Sc galaxy that may be barred. The four most discrepant non-barred AGN, found to the right of the shaded region and with  $M_{\text{bh}} \sim 2 \pm 1 \times 10^7 M_{\odot}$  are galaxies 6, 8, 9 and 57 from Table 1. Galaxy number 6 is poorly resolved, making its morphology difficult to dis-

sect. Galaxy number 8 is an edge-on disk galaxy making it difficult to detect a bar if one exists. The ‘inactive’ galaxy with a SMBH mass of  $\sim 10^9 M_{\odot}$ , which appears ten times greater than the value expected from the relation, is NGC 5252.

We caution that Figures 3b) and 3c) are probably not as strong evidence against a separation of barred and unbarred galaxies as a first inspection would suggest. This is because many of the galaxies with velocity dispersions less than  $80\text{--}90 \text{ km s}^{-1}$  are too faint and/or not well enough resolved for us to identify if a bar is present. However, most galaxies which deviate from the “barless”  $M_{\text{bh}}-\sigma$  relation, in the sense that they have overly-large velocity dispersions, do tend to be barred galaxies. If we have failed to identify bars in the sample with  $\sigma > 85 \text{ km s}^{-1}$ , then correcting this would only increase the population of outlying galaxies that are barred. Among the 68 AGN with  $\sigma > 85 \text{ km s}^{-1}$ , 38 are barred or show some indication of possibly being barred. This equates to 56% of a sample which includes both elliptical and disk galaxies. Only 4 of the 30 non-barred AGN galaxies with  $\sigma > 85 \text{ km s}^{-1}$  display a clear departure to the right of the barless  $M_{\text{bh}}-\sigma$  relation, while roughly half of the 38 barred AGN galaxies are deviant in this manner.

It turns out that this behaviour could have been predicted prior to the confirmation provided here. This is because it was known that a) large scale stellar bars are much more common in narrow line Seyfert 1 galaxies than broad-line Seyfert 1 galaxies (Crenshaw et al. 2003; Deo et al. 2006) and that b) narrow-line Seyfert 1 galaxies are observed to reside rightward of the  $M_{\text{bh}}-\sigma$  relation traced by broad-line Seyfert 1 galaxies (Mathur et al. 2001; Wandel 2002; Grupe & Mathur 2004; Mathur & Grupe 2005b).

For the 82 non-barred galaxies — taken from the inactive sample of 50 galaxies plus the sample of 88 active galaxies — the (symmetrical) bisector BCES regression analysis gives the relation

$$\log(M_{\text{bh}}/M_{\odot}) = (8.18 \pm 0.05) + (4.05 \pm 0.18) \log[\sigma/200 \text{ km s}^{-1}], \quad (1)$$

with an r.m.s. scatter of 0.42 dex in the  $\log M_{\text{bh}}$  direction. The slope of this relation is shallower than the (symmetrical)  $M_{\text{bh}}-\sigma$  relations presented by Ferrarese & Merritt (2000) and Ferrarese & Ford (2005), the latter reporting a slope of  $4.86 \pm 0.43$ . Obviously from Figure 3, the exclusion of barred galaxies results in the shallower slope reported here. A slope of 4.24 is obtained when we include all the galaxies.

Using the (non-symmetrical) ordinary least squares regression within the BCES routine which minimises the scatter in the  $\log M_{\text{bh}}$  direction, and is therefore preferred for predicting SMBH masses, one obtains the expression

$$\log(M_{\text{bh}}/M_{\odot}) = (8.15 \pm 0.05) + (3.89 \pm 0.18) \log[\sigma/200 \text{ km s}^{-1}]. \quad (2)$$

This regression does however yield a comparable r.m.s. scatter of 0.41 dex in the  $\log M_{\text{bh}}$  direction. Using the two other routines from Section 3.1 produces a consistent result. While this “barless” relation is also consistent with the previous (non-symmetrical)  $M_{\text{bh}}-\sigma$  relations presented by Gebhardt et al. (2000) and Tremaine et al. (2002), the latter reporting a slope of  $4.02 \pm 0.32$ , equation 2 has been derived using 82 non-barred galax-

ies rather than 31 barred and barless galaxies and is not applicable to barred galaxies. While inclusion of the barred galaxies results in the relation  $(8.03 \pm 0.05) + (3.94 \pm 0.19) \log[\sigma/200 \text{ km s}^{-1}]$ , with an r.m.s. scatter of 0.47 dex, this overlooks the fact that the scatter is not uniformly distributed about this relation. A more reliable estimate of the SMBH masses in barred galaxies would come from a subtraction of 0.3 dex from the barless  $M_{\text{bh}}-\sigma$  relation’s prediction, i.e. dividing by two, and assigning an uncertainty of  $\sim 0.4$  dex.

### 3.3. Third parameters

The presence of a bar can, but does not necessarily, result in a galaxy residing significantly off the barless  $M_{\text{bh}}-\sigma$  relation. Given that, at a fixed velocity dispersion, the range in SMBH mass spans a factor of  $\sim 50$  when considering both non-barred and barred galaxies, it is obviously neither desirable nor optimal to use a single  $M_{\text{bh}}-\sigma$  relation for all galaxy types. The predictive power of such a relation would be too weak for practical purposes.

While the “barless  $M_{\text{bh}}-\sigma$  relation” is useful for non-barred galaxies, in order to accommodate the barred galaxies it would be advantageous if one could identify a third parameter which could account for their offset nature. While barred galaxies do have smaller bulges than large elliptical galaxies, the use of effective half-light bulge radii as a third parameter may only serve to complicate matters. This is because non-barred galaxies with equally small bulge sizes do not deviate from the locus of points defining the barless  $M_{\text{bh}}-\sigma$  relation and thus bulge size is not the reason why the barred galaxies appear offset. Obviously though, plotting the  $M_{\text{bh}}-\sigma$  residuals against bulge size will yield a trend, and this has led some to (perhaps prematurely) conclude that a SMBH “fundamental plane” involving  $M_{\text{bh}}$ ,  $\sigma$  and  $R_e$  exists (see Feoli & Mele 2007; Aller & Richstone 2007; Hopkins et al. 2007). Nonetheless, if the virial expression  $M_{\text{bulge}} \propto \sigma^2 R_e$  roughly produces bulge masses, and  $M_{\text{bh}}$  is related to  $M_{\text{bulge}}$ , then one should expect the addition of  $R_e$ , as initially done by Marconi & Hunt (2003), to make sense. However for pure elliptical galaxies the addition of  $R_e$  appears to offer no benefit (Graham 2008a) and thus further undermines the value of  $R_e$  as a potential third parameter. We feel that more galaxy structural data may be needed to resolve this issue.

Graham (2008a) speculated that the offset nature of the barred galaxies may be related to an increased exposure to the radial orbits of stars in bars. If this is the case, then one would expect that the bars in more inclined (i.e., edge-on) galaxies will, in general, have increased velocity dispersions if the bars are orientated toward us. Of course an edge-on galaxy may still have a bar which is aligned along the plane of the sky, yielding no increase to the observed velocity dispersion. Nonetheless, to probe this idea we can use the inclination of the disks, traced by the ellipticity of their outer isophotes. The inclinations,  $i$ , of the disk galaxies are of course related to their observed ellipticities via  $\cos(i) = (1 - \epsilon)$ , which were themselves obtained from the IRAF routine ELLIPSE and are listed in Table 1. The data in Figure 4, which shows the vertical residuals about the “barless  $M_{\text{bh}}-\sigma$ ” for the barred galaxies, plotted against the apparent disk

ellipticity ( $\epsilon$ ), are not particularly supportive of this scenario as they do not reveal a distribution of residuals which broadens at larger ellipticities.

The near uniform distribution of points in Figure 4 suggests that something other than disk inclination may be at play. As noted by Gadotti & Kauffmann (2009), it could be the age of the bar such that older bars have had time to increase the central velocity dispersion and thereby drive galaxies off the barless  $M_{\text{bh}}-\sigma$  relation. Indeed, Perez et al. (2009) have reported that older bars have greater velocity dispersions than younger bars. They also note that older bars have positive metallicity gradients. Unfortunately, such diagnosis requires spatially resolved spectral information which is not trivial to acquire, and therefore difficult to implement as a practical third parameter to reduce the scatter in the  $M_{\text{bh}}-\sigma$  diagram.

## 4. SUMMARY AND COMMENTARY

A number of immediate observations can be made from the  $M_{\text{bh}}-\sigma$  diagram shown in Figure 3. (1) While AGN have a reputation for displaying a greater level of scatter in the  $M_{\text{bh}}-\sigma$  diagram than inactive galaxies, this is primarily because the AGN sample contains many barred galaxies. That is, the greater uncertainty from (reverberation mapping and emission line)-derived black hole masses, compared to direct measurements, is not the main cause of the increased scatter in the  $M_{\text{bh}}-\sigma$  diagram. (2) The barred galaxies, in the current sample of 138 galaxies, tend not to have SMBH masses greater than  $10^8 M_{\odot}$ . (This is in part a reflection on the maximum masses of bulges in disk galaxies.) (3) To the left of the shaded region in Figure 3b, galaxies tend not to be barred, while to the right of the shaded region most of the galaxies are barred.

This structure within the  $M_{\text{bh}}-\sigma$  plane inhibits the accuracy to which black hole masses can be predicted in other (barred) galaxies for which only the velocity dispersion is known. While for elliptical and barless disk galaxies one can still obtain an accurate estimate using the “barless  $M_{\text{bh}}-\sigma$  relation” (equation 2), the situation is less favourable for the barred galaxies. It may be that dynamically old bars have increased the central velocity dispersion in these galaxies.

The obvious consequence of this work is that the galaxy velocity dispersion is not the sole driving force which determines the masses of black holes at the centres of galaxies. It is also apparent that dividing one’s sample into elliptical and disk galaxies is not an appropriate approach to take as this would come at the expense of accurate SMBH masses for non-barred disc galaxies.

Barred galaxies do not appear as outliers in current relations involving black hole mass and spheroid luminosity (Graham 2008a, his figure 3; Bentz et al. 2009). Increasing the sample sizes used in these diagrams, which has currently been limited to only 20 to 30 objects, is recommended. Acquiring deeper, higher-resolution, near-infrared images than 2MASS would be a valuable step forward toward better understanding the driving forces that dictate the masses of supermassive black holes at the centres of galaxies.

It should also be insightful to determine, in subsequent work, the scaling factor (e.g., Onken et al. 2004) which brings reverberation-based SMBH masses for non-

barred AGN into better agreement with the barless  $M_{\text{bh}}-\sigma$  relation for quiescent galaxies. The prevalence of barred AGN in such past analyses may have skewed these measurements and hindered constraints for the different

broad-line region models. Ongoing and future observing reverberation mapping campaigns may therefore like to consider focussing on non-barred AGN for which the velocity dispersion is, or can be readily, acquired.

## REFERENCES

- Akritas, M.G., & Bershadsky, M.A., 1996, *ApJ*, 470, 706  
 Aller, M.C., & Richstone, D.O. 2007, *ApJ*, 665, 120  
 Abazajian, K., et al. 2008, *ApJS*, submitted (arXiv:0812.0649)  
 Bentz, M., Peterson, B.M., Pogge, R.W., Vestergaard, M. 2009, *ApJ*, 694, L166  
 Crenshaw, D.M., Kraemer, S.B., & Gabel, J.R. 2003, *AJ*, 126, 1690  
 Deo, R.P., Crenshaw, D.M., & Kraemer, S.B. 2006, *AJ*, 132, 321  
 Erwin, P., & Sparke, L.S. 2002, *AJ*, 124, 65  
 Eskridge, P.B., et al. 2000, *AJ*, 119, 536  
 Feoli, A., & Mele, D. 2005, *Int. Jour. Mod. Phys. D*, 16, 1261  
 Ferrarese, L., & Ford, H.C. 2005, *Space Science Reviews*, 116, 523  
 Ferrarese, L., & Merritt, D., 2000, *ApJ*, 539, L9  
 Ferrarese, L., Pogge, R.W., Peterson, B.M., Merritt, D., Wandel, A., & Joseph, C.L. 2001, *ApJ*, 555, L79  
 Forbes, D.A., Norris, R.P., Williger, G.M., & Smith, R.C. 1994, *AJ*, 107, 984  
 Gadotti D.A., & de Souza R.E. 2005, *ApJ*, 629, 797  
 Gadotti D.A., & Kauffmann, G. 2009, *MNRAS*, submitted (arXiv:0811.1219)  
 Gebhardt, K., et al. 2000, *ApJ*, 539, L13  
 Graham, A.W. 2007, *Bulletin of the American Astronomical Society*, 38, 759 (#13.27)  
 Graham, A.W. 2008a, *ApJ*, 680, 143  
 Graham, A.W. 2008b, *PASA*, 25, 167 (arXiv:0807.2549)  
 Greene, J.E., & Ho, L.C. 2005, *ApJ*, 630, 122  
 Greene, J.E., & Ho, L.C. 2006, *ApJ*, 641, L21  
 Grupe, D., Mathur, S. 2004, *ApJ*, 606, L41  
 Hernández-Toledo, H.M., Vázquez-Mata, J.A., Martínez-Vázquez, L.A., Avila Reese, V., Méndez-Hernández, H., Ortega-Esbrí, S., & Núñez, J.P.M. 2008, *AJ*, 136, 2115  
 Hopkins, P.F., Hernquist, L., Cox, T.J., Robertson, B., & Krause, E. 2007, *ApJ*, 669, 67  
 Hu, J. 2008, *MNRAS*, 386, 2242  
 Jerjen, H., Kalnajs, A., & Binggeli, B. 2000, *A&A*, 358, 845  
 Kaspi, S., Maoz, D., Netzer, H., Peterson, B.M., Vestergaard, M., & Jannuzi, B.T. 2005, *ApJ*, 629, 61  
 Kelly, B.C. 2007, *ApJ*, 665, 1489  
 Knapen, J.H., Shlosman, I., & Peletier, R.F. 2000, *ApJ*, 529, 93  
 Krolik, J. H. 2001, *ApJ*, 551, 72  
 Marconi, A., & Hunt, L. 2003, *ApJ*, 589, L21  
 Marinova, I., & Jogee, S. 2007, *ApJ*, 659, 1176  
 Mathur, S., Grupe, D. 2005a, *A&A*, 432, 463  
 Mathur, S., Grupe, D. 2005b, *ApJ*, 633, 688  
 Mathur, S., Kuraszewicz, J., & Czerny, B. 2001, *NewA*, 6, 321  
 Metzroth, K.G., Onken, C.A., & Peterson, B.M. 2006, *ApJ*, 647, 901  
 Novak, G.S., Faber, S.M., Dekel, A., 2006, *ApJ*, 637, 96  
 Onken, C.A., Ferrarese, L., Merritt, D., Peterson, B.M., Pogge, R.W., Vestergaard, M., & Wandel, A. 2004, *ApJ*, 615, 645  
 Perez, I., Sanchez-Blazquez, P., Zurita, A. 2009, *A&A*, 495, 775  
 Press, W.H., Teukolsky, S.A., Vetterling, W.T., & Flannery, B.P., 1992, *Numerical recipes* (2nd ed.; Cambridge: Cambridge Univ. Press)  
 Tremaine, S., et al., 2002, *ApJ*, 574, 740  
 Vestergaard, M., & Peterson, B.M. 2006, *ApJ*, 641, 689  
 Wandel, A. 2002, *ApJ*, 565, 762  
 Wang, T., & Lu, Y. 2001, *A&A*, 377, 52  
 Weinzierl, T., Jogee, S., Khochfar, S., Burkert, A., & Kormendy, J. 2009, *ApJ*, in press (arXiv:0807.0040)  
 Yuan, C., Yen, D.C.C., & Li, I.-H. 2001, *BAAS*, 33, 1483 (#118.02)  
 Zhou, H., Wang, T., Yuan, W., Lu, H., Dong, X., Wang, J., & Lu, Y. 2006, *ApJS*, 166, 128

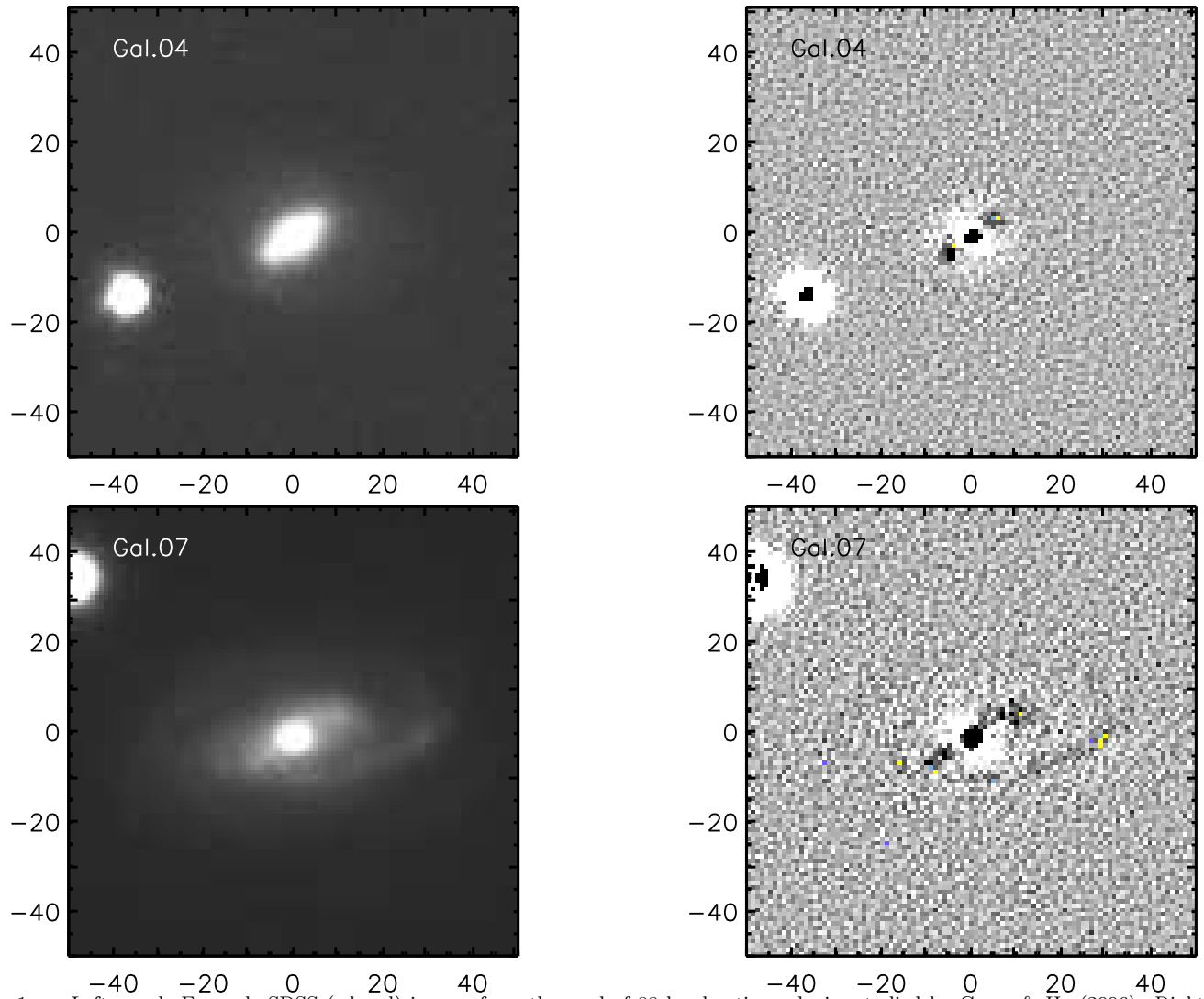


FIG. 1.— Left panel: Example SDSS (r-band) images from the pool of 88 local active galaxies studied by Green & Ho (2006). Right panel: Unsharp masking helps to reveal the presence of bars. The axis tick marks denote pixels, which correspond to a size of 0.396 arcseconds. Image pairs for all 88 galaxies are available via the electronic version of this paper. Note: The positive/negative (white/black) has been reversed in the residual images.



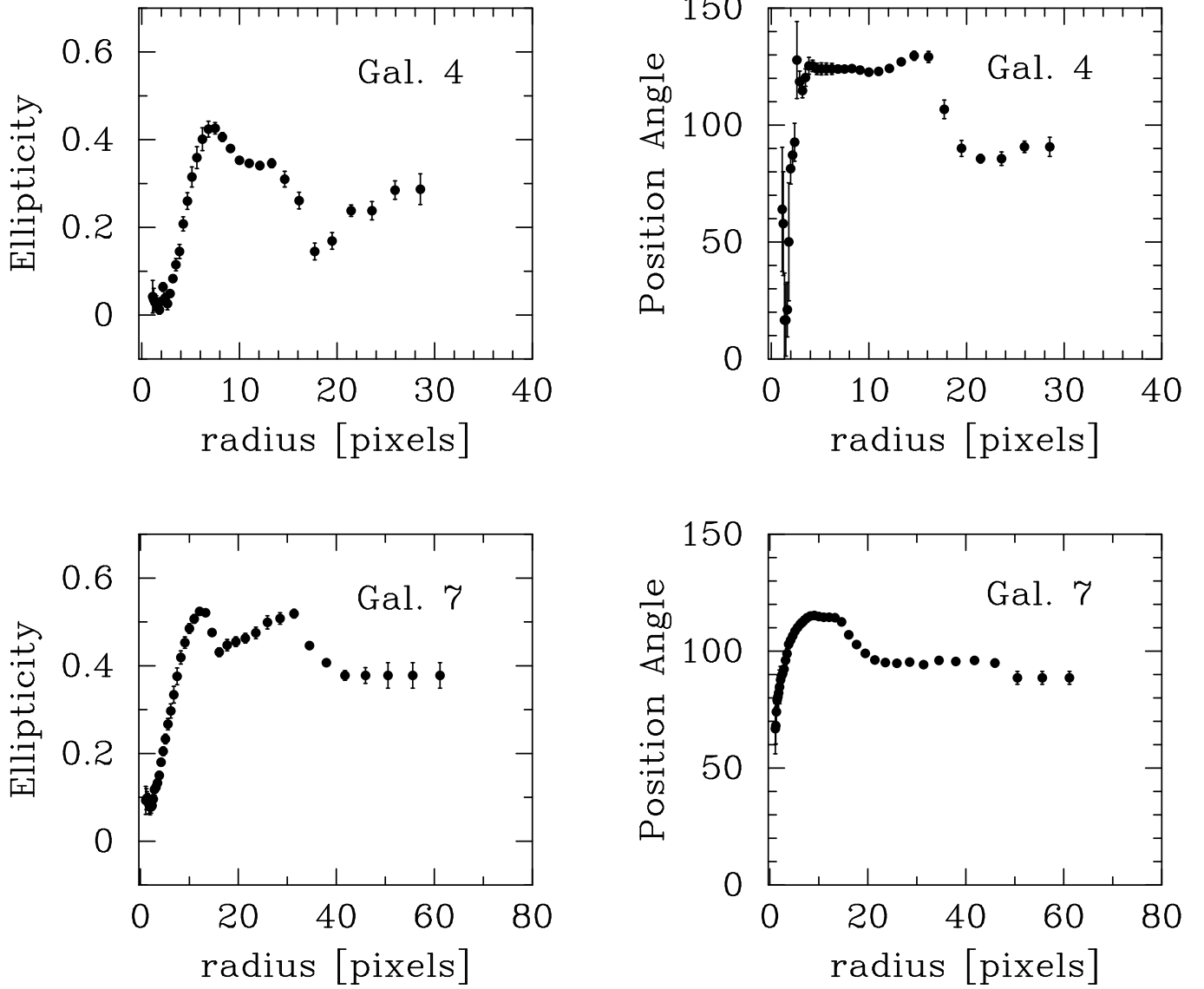


FIG. 2.— Ellipticity and position angle profiles for the galaxies shown in Figure 1

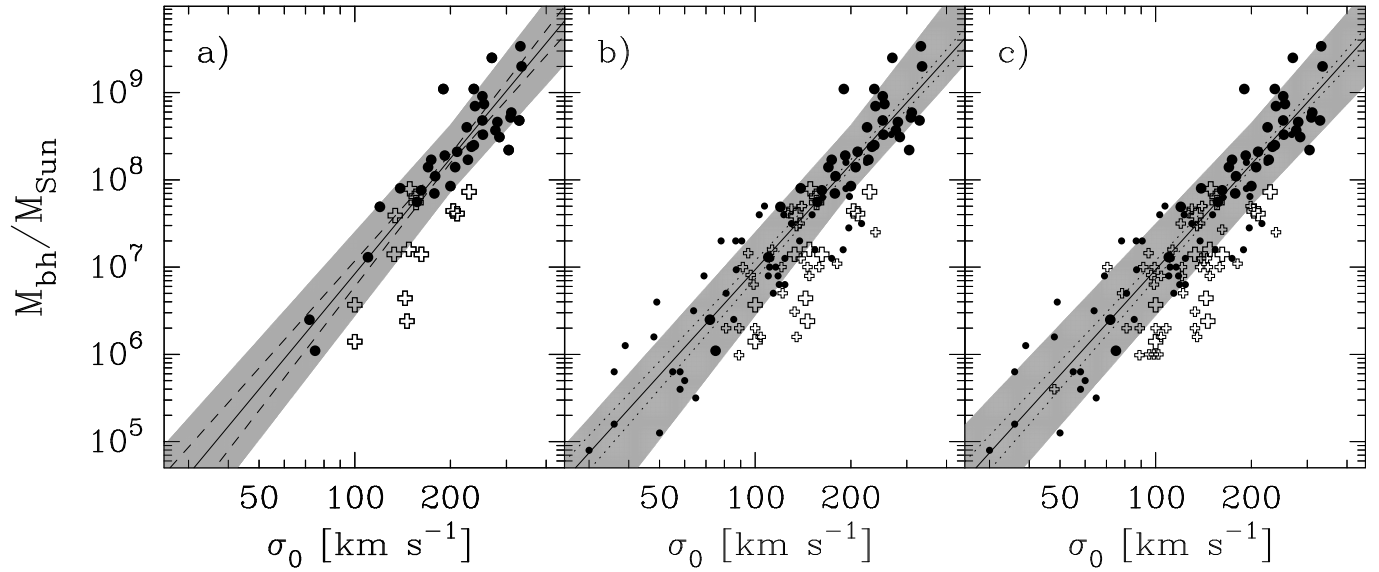


FIG. 3.—  $M_{\text{bh}}-\sigma$  diagram. Crosses denote galaxies with (suspected) bars. Panel a) shows 50 galaxies with direct SMBH mass measurements, as tabulated by Graham (2008b, his Table 1). The solid line shows the (symmetrical) linear regression to the 36 non-barred galaxies, while the dashed lines delineate the  $1\sigma$  uncertainty for this relation. The shaded area extends this boundary by 0.33 dex in the  $\log M_{\text{bh}}$  direction. The outlier at the high-mass end with  $M_{\text{bh}} = 10^9 M_{\odot}$  is NGC 5252, Panel b) includes the AGN from Table 1 which are designated as either having a bar or not having a bar. While the shaded region has been kept the same as in panel a) for comparison purposes, the solid line shows the (symmetrical) linear regression to the 82 non-barred galaxies, while the dotted lines delineate the  $1\sigma$  uncertainty for this relation. Panel c) additionally includes those AGN for which there may be a bar; that is, systems designated as “maybe” are treated as “yes” in this panel (see Table 1). The shaded region extends the boundary around the dotted lines by 0.42 dex — which is the r.m.s. scatter about the barless  $M_{\text{bh}}-\sigma$  relation for the 82 non-barred (AGN and inactive) galaxies.

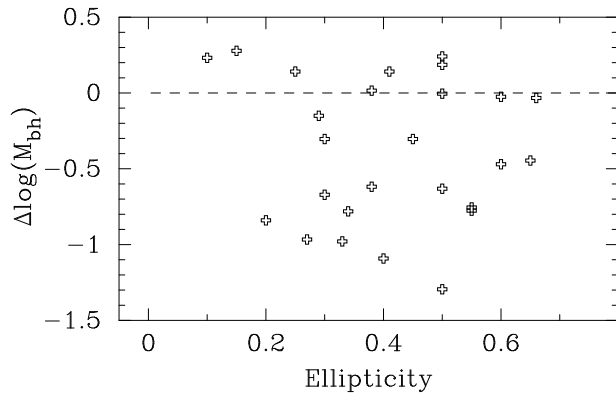


FIG. 4.— Vertical residuals of the barred galaxies about the barless  $M_{\text{bh}}-\sigma$  relation shown in Figure 3b plotted against the ellipticity of each galaxy’s outer isophotes — a measure of their disk’s inclination.